PAPER

Check for updates

Effects of alkanolamine solvents on the aggregation states of reactive dyes in concentrated solutions and the properties of the solutions

Chuangui Cao,†[a] Zhihui Zhao,†[a] Yong Qi,[a] Hui Peng,[a] Kuanjun Fang,[ab] Ruyi Xie[*ab] and Weichao Chen [iD] [*ab]

The aggregation of dyes is a common phenomenon in solutions, particularly concentrated solutions, which seriously affects the dyeing and printing processes. In this study, the effects of alkylamine solvents on the reactive dye aggregation behavior in highly concentrated solutions was studied. Typical cases were conducted with two slightly toxic and environmentally friendly solvents, namely diethanolamine (**DEA**) and triethanolamine (**TEA**), and two reactive dyes, namely C. I. Reactive Red 218 (**R-218**) and C. I. Reactive Orange 13 (**O-13**). Aggregation states were studied by ultraviolet-visible (UV-Vis) absorption spectroscopy, Gaussian-peak-fitting method and fluorescence spectroscopy. The results showed that both the additives **DEA** and **TEA** could reduce the dye aggregation because the solvents, **DEA** and **TEA**, can break the iceberg structure and allow easy entry of the molecules into the dye aggregates. Also, the disaggregation caused by **DEA** was higher as compared with **TEA**, which may be caused by the weaker hydrogen bond and the relatively smaller steric hindrance effects of **DEA**. The schematic of disaggregation between **R-218** and **DEA** was also discussed. For **R-218**, the dimers were disaggregated to monomer, while the higher-ordered aggregates were disaggregated to trimers and dimers for **O-13**. Moreover, physical properties such as viscosity and surface tension of the solutions were measured. This investigation is instructive for the further dyeing progress with organic bases in the textile industries.

1. Introduction

The aggregation behavior of small molecules, particularly, dye molecules with planar benzene ring structures usually tend to self-aggregate because of the molecular interactions in solution phase.[1–3] This behavior has an important impact on their applications in textile, biological, colloid and other fields.[4–6] Among the various types of dyes, azo reactive dyes used for cellulose fiber dyeing and printing have drawn special attention because of their variety and bright color. However, reactive dyes tend to aggregate in solutions due to their good planarity.[7,8] When dye molecules are dissolved in water, the hydrophilic parts tend to attract water, while the aromatic rings of azo reactive dyes overlap to form a stack due to the π–π interaction; therefore, the water molecules form a hydration layer *via* hydrogen bonds around the stack,[9,10] which is known as Frank's iceberg.[11] During the process of dyeing and printing, auxiliaries are generally added to improve the fixing

and printing effects.[12] The additives are mainly used for increasing the solubility and adjusting the properties of the dye solution to improve printing effects.[13–15] Moreover, the adsorption and diffusion of dyes can be affected by the aggregation state. In the process of dyeing, inorganic bases are commonly used for the fixing process, but the interactions between alkanolamine solvents and the aggregation state are not clear in concentrated solutions. Therefore, it is quite necessary to study the interactions between the alkanolamine solvents and azo reactive dyes on the aggregation behavior and the dye solution properties in the concentrated solution in order to guide the future dyeing research.

The aggregation states are also influenced by the solution environments, such as the other additives. The addition of urea, ethanol and pyridine in the dye solution reduces the degree of dye aggregation.[9,10,16] However, previous reports mainly focused on the study of aggregation states in dilute solutions; however, in dye industries, concentrated dye solutions are often used. Therefore, it is necessary to investigate the aggregation state of dye molecules in concentrated solutions. Water-soluble polymers[17–19] and additional organic solvents, such as lactam compounds, ethylene glycol can obtain better inkjet printing effects[20–23] because these are mainly used to reduce the formation of satellite droplets at high concentrations. The aggregation behavior is also affected by salts, particularly, by the metal

[a]College of Textiles & Clothing, State Key Laboratory of Bio-Fibers and Eco-Textiles, Collaborative Innovation Center for Eco-Textiles of Shandong Province, Qingdao University, Qingdao 266071, China. E-mail: chenwc@qdu.edu.cn

[b]National Manufacturing Innovation Center of Advanced Dyeing and Finishing Technology, Tai'an 271001, China

† These authors contributed equally to this work.

ion salts in solutions. Ravishanker[24] and Herz et al.[25] reported that the "iceberg" structure of neighboring dye molecules was destroyed by electrolytes, leading to the enhancement in the degree of dye aggregation. Mostafa et al.[10] found that the length and cross section of the Acidic Red 266 aggregates increased significantly and the aggregation of Reactive Red 9 and Orange 13 were both enhanced in the presence of electrolytes in dye solutions.[26] In the dyeing process, the addition of inorganic bases may also cause the dye aggregation. Moreover, an important factor in the dyeing process is the rapid diffusion of dye molecules into the fiber, a process that requires maximum disaggregation of the dye aggregates. In addition, the adsorption and diffusion of dye molecules into the fiber are also related to the properties of the dye solution. Therefore, the aggregation states and the physical parameters, viscosity and surface tension of the dye solution play an important role for their application in the textile field. Therefore, it is necessary to study the interactions between organic bases and azo reactive dyes on the properties and aggregation states of the dye solution.

Alkali conditions are essential for the fixation of reactive dyes. Inorganic bases are mainly used in traditional dyeing, but they are usually consumed in a great quantity, causing defects in textiles during the traditional production of dyeing. Here, two alkali alkanolamine solvents, namely diethanolamine (**DEA**) and triethanolamine (**TEA**), were added into the concentrated solutions of two azo reactive dyes, namely C. I. Reactive Red 218 (**R-218**) and C. I. Reactive Orange 13 (**O-13**). The effects of the solvents to the aggregation states of dyes were investigated *via* ultraviolet-visible (UV-Vis) absorption spectroscopy, Gaussian-peak-fitting and fluorescence spectroscopy. Properties such as surface tension and viscosity of dye solutions were also investigated. Results revealed that additional **DEA** and **TEA** could suppress the aggregation of **R-218** and **O-13** through the hydrophobic effects of **DEA** and **TEA**. The different aggregation states for **R-218** and **O-13** solutions could have been the result of different effects among numerous dye/solvent combinations of the dyes' chemical structures and physical properties of the solvents. The smaller space steric hindrance of dye molecules, lower hydrogen bonding force, and smaller space steric hindrance of the solvent could also reduce the dye aggregation states. In addition, the surface tension and viscosity of dye solutions also changed by the aggregation behaviour of the two dyes and physical properties of the solvents. These results are instructive for advancing the dyeing progress.

2.   Experimental

2.1   Materials

High-purity **R-218** and **O-13** were supplied by Everlight Chemical Industrial Corporation. **TEA** and **DEA** (AR 99%) were provided by Shanghai Aladdin Biochemical Technology Co. Ltd. Ultra-pure water with a resistivity of 18.2 MΩ cm at 25 °C was used throughout the experiment. The structures of the two dyes (**R-218** and **O-13**) and two additional solvents (**DEA** and **TEA**) are displayed in Fig. 1.
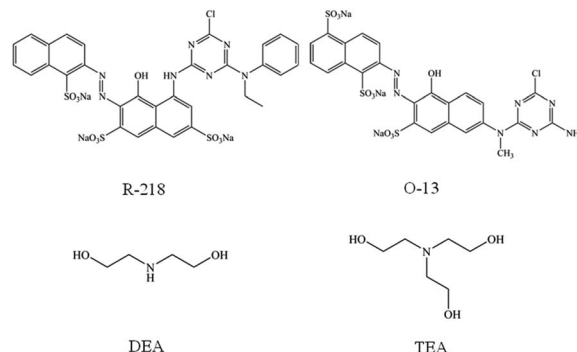

Fig. 1   Molecular structures of **R-218**, **O-13**, **DEA** and **TEA**.

2.2   Preparation of the concentrated solutions

1 wt%, 2 wt%, 3wt%, 4wt% and 5wt% aqueous solutions (aq) of **DEA** and **TEA** were prepared, respectively, and then were used to dissolve **R-218** and **O-13** to the uniform concentration of 1 mM and 100 mM. **R-218/O-13** dissolved in pure water with the concentration for 10 mM, 20 mM, 50 mM and 100 mM were also prepared.

2.3   Measurements

UV-vis absorption spectroscopy was performed on an AU-3900H UV spectrophotometer (Hitachi High-tech Co, Ltd, Tokyo, Japan). A micro-cuvette with an optical path of 0.01 mm was used to escape high concentration-induced analysis errors.

Fluorescence spectroscopy was performed on an FS5 Fluorescence Spectrometer (Edinburgh Instruments Ltd, Kirkton Campus, UK) at 25 °C.

Dynamic surface tension was measured by a Bubble Pressure Tensiometer BP-100 (Bubble Pressure Tensioeter company, KRUSS, Germany) at 25 °C.

The viscosity of the samples was recorded using a FLUDI-CAM RHEO microfluidic visual rheometer (Formulaction company, Toulouse, France) at 25 °C.

3.   Results and discussions

3.1   UV-vis absorption spectroscopy

The UV-vis absorption spectroscopy is the most commonly used method to understand the changes in dye aggregation states in solutions.[27–29] It has been found that dye aggregation can be split into two main types: one is the blue-shift observed in the dimer peak relative to the monomer peaks that form H-aggregates, and the other is J-aggregates, conversely.[30–33] Fig. 2a and b show that the UV-vis absorption spectra of **R-218**
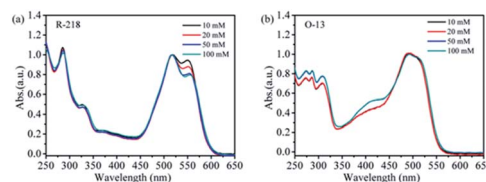

Fig. 2   The UV-vis absorption spectra of the two dye aqueous solutions with different concentrations, (a) **R-218**, (b) **O-13**.

and **O-13** with different concentrations in aqueous solutions, respectively. According to their specific molecular structures, both **R-218** and **O-13** tend to form face-to-face parallel arrangements (H-aggregates) by π–π stacking interactions of the planar parts. For this type of aggregation, the maximum UV-vis absorbance peak of the aggregates is blue-shifted compared to the monomer.[34,35] For **R-218**, the peaks at 555 nm and 518 nm belonged to the absorption of monomers and dimers, respectively, and the shoulder peaks around 480 nm belonged to the higher-ordered aggregates. Similarly, for **O-13** (Fig. 2b), the peaks at 520 nm, 478 nm and around 400 nm belonged to monomers, dimers, and higher-order aggregates, respectively. For the two dyes, the changes in the peaks indicated variation in the aggregation states. Obviously, for **R-218**, with the increase in the dye concentration, the absorption intensity at the monomer peak gradually decreased. For **O-13**, the intensity of higher-ordered aggregates increased. That may be due to the increase in the number of dye molecules in the dye solution, resulting in the increase in entropy, and the chance of collision between dye molecules was increased, thus, the aggregation of dye molecules was enhanced.

Fig. 3 shows the UV-vis absorption spectra of **R-218** and **O-13** in aqueous solutions and different concentrations of **DEA/TEA**. All spectra were normalized with respect to the maximum absorption peak. For **R-218**, the absorbance of monomers gradually increased with the increase in the **DEA/TEA** concentration. It indicated that **DEA** and **TEA** caused the disaggregation of **R-218** in the solutions. Moreover, the degree of disaggregation influenced by **DEA** was much larger as compared to **TEA**. However, for **O-13**, the absorption of monomers barely changed, but the peaks of aggregates (350–450 nm) changed regularly with the increasing concentration of **DEA**. The spectra of **O-13**/**TEA** combination had no obvious changes. In order to investigate further the quantitative changes in dye aggregation states in different solutions, Gaussian-peak-fitting of the spectra was conducted.

We calculated **DEA/TEA** with a mass ratio of 1–5% into the moles, which is more conducive to quantitatively compare the changes in the two dye aggregate states; λ_m/λ_d and λ_m/λ_h are the intensities of the UV-vis absorption spectra between the
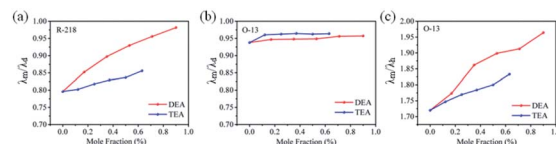

Fig. 4 The intensity of the UV-vis absorption spectra of R-218 (a) and O-13 (b and c) in the same mole of DEA and TEA. (a) The λ_m/λ_d of R-218, (b) the λ_m/λ_d of O-13, (c) the λ_m/λ_h of O-13.
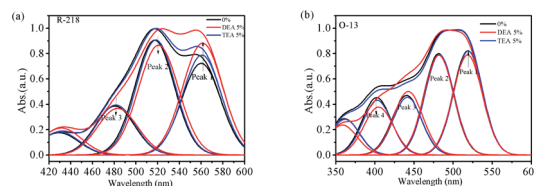

Fig. 5 Gaussian-peak-differentiating-imitating curves of the UV-vis absorption spectra of R-218 (a) and O-13 (b) in different solvents.

monomer peak (λ_m) and the dimmers (λ_d) and the higher-ordered aggregates (λ_h), respectively. It can be seen from Fig. 4a that for **R-218** the intensity of λ_m/λ_d gradually increased with the increase in the mole content of **DEA/TEA**, and the λ_m/λ_d of **DEA** is higher compared to that of **TEA** with the same mole content in the dye solution. From the same calculation, for **O-13** (Fig. 4b and c), it also can be also seen that with the increasing in the mole ratio of **DEA/TEA**, the ratio of λ_m/λ_d showed slight variations, while the ratio of λ_m/λ_h changed significantly. When the same moles of **DEA/TEA** were added to the dye solution, additional changes in **DEA** were higher as compared to **TEA**. This result shows that **DEA** has better performance in inhibiting the dye aggregation compared to **TEA**; these changes are also consistent with the results in UV-vis absorption spectroscopy.

3.2 Gaussian-peak-fitting curves

Fig. 5 shows the Gaussian-peak-fitting curves. All the fitting coefficients were larger than 99.99%. The fitting curves of **R-218** and **O-13** were divided into 3 peaks and 4 peaks, respectively. Peak 1 of each curve corresponded to the dye monomer, while peaks 2–4 corresponded to dimers, trimers, and higher-ordered aggregates, respectively. The integral area of each peak was calculated in the form of proportion as provided in Table 1, which was then used to explore the quantitative changes in the
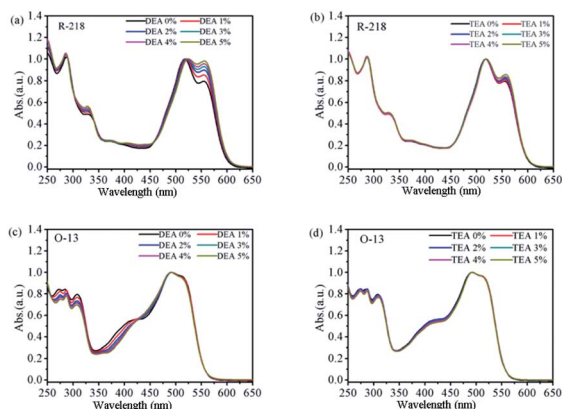

Fig. 3 The UV-vis absorption spectra of R-218 (a and b) and O-13 (c and d) in DEA and TEA solutions with different concentrations.

Table 1 The area proportion of each peak of Gaussian peak-fitting curves

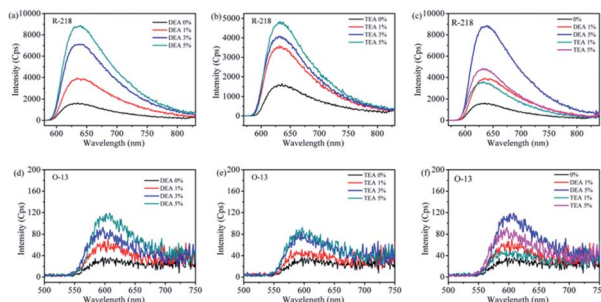| Dyes	Solvents	Area contributions of peaks (%)			
		Peak 1	Peak 2	Peak 3	Peak 4
R-218	0%	32.98	41.33	17.66	
	5% **DEA**	37.86	37.15	15.82	
	5% **TEA**	34.66	39.93	17.41	
O-13	0%	29.06	28.26	16.56	15.96
	5% **DEA**	29.30	29.24	18.56	14.08
	5% **TEA**	29.50	28.51	16.34	15.50

Fig. 6 Fluorescence spectra of **R-218** (a–c) and **O-13** (d–f) in **DEA** and **TEA** solutions with different contents, the concentration of dye solutions is 1 mM.

aggregation states. It can be seen from Table 1 that for **R-218** in a 5% **DEA** solution the proportion of peak 2 (dimer) and peak 3 (trimer) reduced by 20.20% and 10.42%, while the area of peak 1 (monomer) increased by 14.98%. However, the area of peak 2 and peak 3 only reduced by 3.51% and 2.94%, respectively, while that of peak 1 increased by 5.09% in a 5% **TEA** solution. As previously discussed, these results indicated that both the addition of **DEA** and **TEA** lead to the disaggregation of **R-218**; however, **DEA** had much more impact on the disaggregation effect compared to **TEA**. In addition, for **R-218**, the disaggregation effects on dimers were larger compared to higher-ordered aggregates. For **O-13** in the 5% **DEA** solution, the proportion of peak 4 (higher-ordered aggregates) decreased by 11.78%, while peak 3 (trimer), peak 2 (dimer) and peak 1 (monomer) increased by 12.08%, 3.47% and 0.83%, respectively. This result suggested that **DEA** caused the disaggregation of higher-ordered aggregates mainly into trimers rather than in dimers and monomers. The aggregation states of **O-13** in the 5% **TEA** solution changed a little, but a positive effect could still be observed. These different changes in the aggregation states of **R-218** and **O-13** were due to the distinct molecular structures of the two dyes. As shown in Fig. 1, the non-conjugated part for **R-218** was located at the α-position of the naphthalene ring, while is situated at the β-position for **O-13**. Therefore, the steric hindrance of **O-13** molecules is smaller than of **R-218**. That is
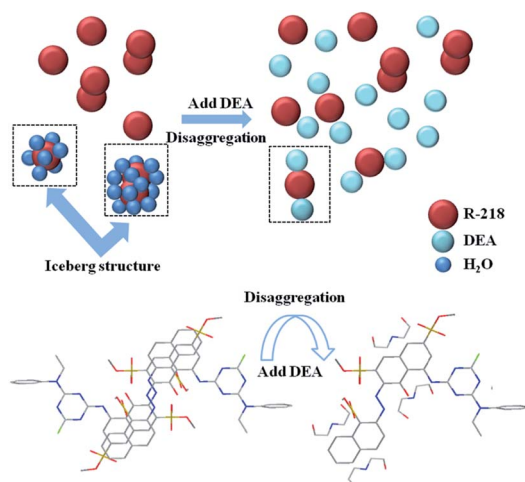
why bigger aggregates were much easier to observed in **O-13** solutions. It was also the reason for the disaggregation of **O-13** that occurred in higher-ordered aggregates.

3.3 Fluorescence spectroscopy

Fluorescence spectroscopy is also an important measure to analyze the aggregation state of dyes.[36,37] The increasing degree of dye aggregation could reduce the intensity of fluorescence.[38] As shown in Fig. 6a and b, for **R-218**, the fluorescence intensity gradually increased with the increase in the concentration of **DEA/TEA** in dye solutions. Fig. 6c, the fluorescence intensity of **R-218** with **DEA** is higher compared to that of **TEA**. The change in the fluorescence intensity was consistent with the ultraviolet absorption spectra (Fig. 3a and b). These results showed that both the addition of **DEA** and **TEA** could reduce the degree aggregation of **R-218**, and **DEA** had a bigger impact on the disaggregation effects compared to **TEA**. For **O-13**, as shown in Fig. 6d–f, the fluorescence intensity also increased with the increase in the **DEA/TEA** content in dye solutions, and the intensity with **DEA** was higher compared with that of **TEA**. However, the fluorescence intensities of **O-13** and **R-218** with 5% **DEA** were 115 and 8790, respectively, which indicate that the highest disaggregation was observed to the **R-218/DEA** combination. These results are consistent with the UV-vis absorption spectra (Fig. 3 and 5).

3.4 The interactions between R-218 and DEA

Hydrogen bonds and hydrophobic forces in the hydrophobic parts of dye molecules lead to different degrees of dye aggregation.[38] It has been pointed out that the hydration layer around the benzene ring consists of 24 water molecules.[24]

The interactions between the dyes and the solvents were also studied by taking the most significant combination (**R-218** in 5% **DEA** solution) as an example. Fig. 7 shows the possible schematic of the different aggregation states. Before the addition of **DEA**, there were monomers, dimers and higher-ordered aggregates present in the solution. Dye molecules stack *via* π–π interactions with a better planarity from the benzene ring and naphthalene ring, thus resulting in dye molecules to form dimers or higher-ordered aggregates. H-type aggregates exist in the solution due to face-to-face stacking. The water molecules surround the dye molecules with different aggregation states by hydrogen bonding. However, after the addition of **DEA**, the hydrophobic parts of dye molecules and the **DEA** molecules attracted by each other. First, the "iceberg structure" water around **R-218** aggregates got destroyed; then, the water molecules that originally surrounded the dye aggregates were released; further, the naphthalene ring part of **R-218** molecules was packaged by the hydrophobic part of the **DEA** molecules and the hydrophilic part of **DEA** molecules was exposed to the water, which resulted in the naphthalene ring hydrophilic. As a result, the hydrophilic group of **DEA** molecules surround the dye molecules, which could interact with the water molecule through hydrogen bonds resulting in the formation of a hydration layer. As a consequence, the disaggregation was achieved. Other dye/solvent combinations went through a similar process

Fig. 7 The interaction between **R-218** and **DEA** in the dye solution.

Paper

RSC Advances

Table 2 Some physical parameters of DEA and TEA

Solvent	Dispersion force	Molar volume	Hydrogen bonding	Relative molecular weight
DEA	17.2	95.5	21.2	105.1
TEA	17.3	133.2	23.3	149.2
H_2O	15.5	42.3		18.0

but to different degrees. The disaggregation effects of different solvents were explained from aspect of the physical properties of the solvents. As listed in Table 2, **DEA** and **TEA** have higher dispersion forces compared to water. This meant that the hydrophobic interactions between **DEA**/**TEA** and the naphthalene ring of dyes were much higher than that of water.

That was the key factor to destroy the "iceberg structure" of aggregates. Then, the steric hindrance effect of **DEA** was lower compared to **TEA** since the molecular volume of **DEA** present was small to interact with the dye, although the dispersion forces of two solvents are roughly equal. Moreover, the relative molecular weight of **DEA** is smaller as compared with **TEA**, so there were more dissociated **DEA** molecules in the solution to interact with the dye molecules and to reduce aggregation.

3.5 Dynamic surface tension

Surface tension of dye solutions plays an important role in the dyeing process.[28,39,40] Reducing the surface tension is beneficial to promote the wetting of the fabric surface and the diffusion of dye molecules into the fibers. Fig. 8 shows the surface tension of **R-218** and **O-13** in different solutions. The surface tension of pure water was also plotted for comparison. The curves of **R-218** solutions were significantly lower compared to that of water (Fig. 8a and b), while those of **O-13** almost overlapped with water. This distinction was caused by the different distribution of hydrophilic groups of **R-218** and **O-13**. The hydrophilic groups are located on one side of **R-218** molecules; therefore, **R-218** molecules could adsorb to the gas–liquid interface of the solution like surfactant to reduce the surface tension. However, the hydrophilic groups of **O-13** are located on both sides, so **O-13** molecules had little effects on the surface tension of the

solution. Despite being obvious or not, the surface tension of all the solutions decreased gradually with the increase in the concentration of **DEA** or **TEA**. That was mainly because the number of dye monomers increased with the increasing amount of the solvent. Moreover, the interactions between **DEA**/**TEA** molecules and water also decreased the surface tension.

3.6 Rheological

Fig. 9 shows that the viscosity-shear rate curves of all the solutions. Viscosity of all the tested solutions did not change with the shear rate, which belonged to Newtonian fluid.[41,42] The viscosity of dye solutions depends mainly on the intermolecular forces. All the viscosities increased with the increase in the concentration of solvents. This could be attributed to the decreasing distance and increasing intermolecular interactions between **DEA**/**TEA** and water with the increase in the number of **DEA**/**TEA** molecules. Fig. 9e shows the comparison of **R-218** and **O-13** in the same solvent concentration. Apparently, the viscosity of **R-218** solutions was larger than that of **O-13** because the molecular volume of **R-218** was larger than that of **O-13**. Moreover, the viscosity of solutions with **TEA** was significantly higher compared with **DEA**. That was because the addition of **DEA** leads to a larger number of dye molecules compared to **TEA**, and the interactions between the extra molecules resulted in the larger viscosity.
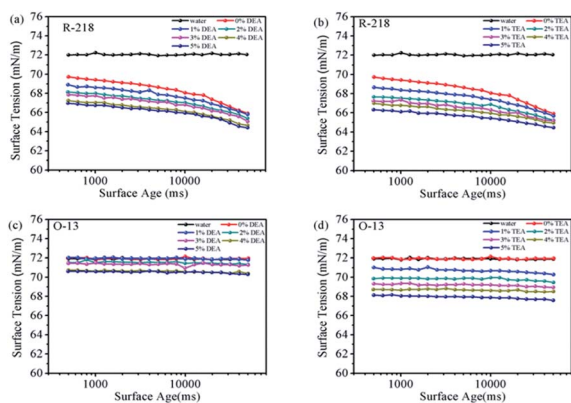

Fig. 8 Dynamic surface tension of **R-218** (a and b) and **O-13** (c and d) in different solutions.
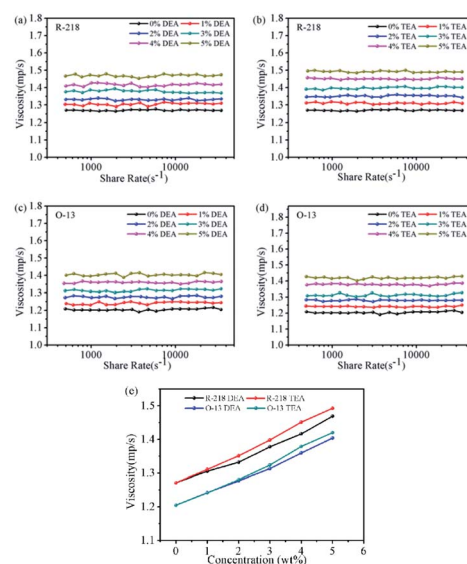

Fig. 9 The viscosity-shear rate curves of **R-218** (a and b) and **O-13** (c and d) in different solutions, (e) plotted viscosity of the dyes *versus* the concentration of the solvents.

4. Conclusions

The effects of the alkanolamine solvent to the aggregation states of reactive dyes in the concentrated solution were investigated. The combinations of **DEA/TEA** and **R-218/O-13** were used for examples. It was the addition of solvents that inspired the disaggregation of the dyes. The change in degree of the aggregation states was quantified. It was found that the highest disaggregation occurred due to the **R-218/DEA** combination. The disaggregation mechanism included the hydrophobic interactions between the hydrophobic parts of the dye, and the solvent destroyed the "iceberg structure" of the aggregates. Then, the different degrees of disaggregation effects were explained from the aspects of the molecular structure of the dye and the physical properties of the solvent. In addition, for the two dyes, the surface tension and viscosity of the solutions were measured. With the increase in the concentration of the solvent in the solutions, the surface tension decreased while the viscosity increased accordingly, which was instructive for future dye applications.

Conflicts of interest

The authors declare no competing financial interest.

Acknowledgements

References

1 F. Jones and D. R. Kent, *Dyes Pigm.*, 1980, **1**, 39–48.
2 A. Navarro and F. Sanz, *Dyes Pigm.*, 1999, **40**, 131–139.
3 K. Murakami, *Dyes Pigm.*, 2002, **53**, 31–43.
4 H. von Berlepsch and C. Bottcher, *Langmuir*, 2013, **29**, 4948–4958.
5 X. Dong, Z. J. Gu, C. Y. Hang, G. Q. Ke, L. W. Jiang and J. X. He, *J. Cleaner Prod.*, 2019, **226**, 316–323.
6 X. Li, G. Huang, W. Chen, H. Jiang, S. Qiao and R. Yang, *ACS Appl. Mater. Interfaces*, 2020, **12**, 16670–16678.
7 H. Wang, H. Kong, J. Zheng, H. Peng, C. Cao, Y. Qi, K. Fang and W. Chen, *Molecules*, 2020, **25**, 1588.
8 L. Zhang, K. Fang and H. Zhou, *Molecules*, 2020, **25**, 2507.
9 K. Hamada, H. Nonogaki, Y. Fukushima, B. Munkhbat and M. Mitsuishi, *Dyes Pigm.*, 1991, **16**, 111–118.
10 O. I. Mostafa, A. Y. Abd El-Aal, A. A. El Bayaa, H. B. Sallam and A. A. Mahmoud, *J. Chin. Chem. Soc.*, 1995, **42**, 507–513.
11 H. S. Frank and M. W. Evans, *J. Chem. Phys.*, 1945, **13**, 507–532.
12 S. M. Burkinshaw and G. Salihu, *Dyes Pigm.*, 2019, **161**, 519–530.
13 H. Wang, H. Kong, J. Zheng, H. Peng, C. G. Cao, Y. Qi, K. J. Fang and W. C. Chen, *Molecules*, 2020, **25**, 9.

14 X. Y. Zhang, K. J. Fang, H. Zhou, K. Zhang and M. N. Bukhari, *J. Mol. Liq.*, 2020, **312**, 113481.
15 L. Zhang, N. Li, F. L. Zhao and K. Li, *Anal. Sci.*, 2004, **20**, 445–450.
16 K. K. Karukstis, L. A. Perelman and W. K. Wong, *Langmuir*, 2002, **18**, 10363–10371.
17 J. Y. Park, Y. Hirata and K. Hamada, *Color. Technol.*, 2012, **128**, 184–191.
18 Z. Y. Tang, K. J. Fang, Y. W. Song and F. Y. Sun, *Polymers*, 2019, **11**, 739.
19 C. Ouyang, S. Chen, B. Che and G. Xue, *Colloids Surf., A*, 2007, **301**, 346–351.
20 K. Ni, H. Fang, Z. Yu and Z. Fan, *J. Mol. Liq.*, 2019, **278**, 234–238.
21 H. Qin, K. Fang, Y. Ren, K. Zhang, L. Zhang and X. Zhang, *ACS Sustainable Chem. Eng.*, 2020, **8**, 17291–17298.
22 R. Y. Xie, K. J. Fang, Y. Liu, W. C. Chen, J. N. Fan, X. W. Wang, Y. F. Ren and Y. W. Song, *J. Mater. Sci.*, 2020, **55**, 11919–11937.
23 H. Peng, R. Xie, K. Fang, C. Cao, Y. Qi, Y. Ren and W. Chen, *Langmuir*, 2021, **37**, 1493–1500.
24 G. Ravishanker, P. K. Mehrotra, M. Mezei and D. L. Beveridge, *J. Am. Chem. Soc.*, 1984, **106**, 4102–4108.
25 A. H. Herz, *Photogr. Sci. Eng.*, 1974, **18**, 323–335.
26 B. Neumann, *J. Phys. Chem. B*, 2001, **105**, 8268–8274.
27 M. G. Bielska, A. Sobczyńska and K. Prochaska, *Dyes Pigm.*, 2009, **80**, 201–205.
28 L. C. Abbott, S. N. Batchelor, J. Oakes, J. R. L. Smith and J. N. Moore, *J. Phys. Chem. B*, 2004, **108**, 13726–13735.
29 B. Boruah, P. M. Saikia and R. K. Dutta, *Dyes Pigm.*, 2010, **85**, 16–20.
30 F. C. Spano, *Acc. Chem. Res.*, 2010, **43**, 429–439.
31 P. Verma and H. Pal, *J. Phys. Chem. A*, 2012, **116**, 4473–4484.
32 A. Eisfeld and J. S. Briggs, *Chem. Phys.*, 2006, **324**, 376–384.
33 E. Rabinowitch and L. F. Epstein, *J. Am. Chem. Soc.*, 2012, **63**, 69–78.
34 Z. Tang, K. Fang, M. N. Bukhari, Y. Song and K. Zhang, *Langmuir*, 2020, **36**, 9481–9488.
35 J. L. Bricks, Y. L. Slominskii, I. D. Panas and A. P. Demchenko, *Methods Appl. Fluoresc.*, 2018, **6**, 1088.
36 T. E. Kaiser, H. Wang, V. Stepanenko and F. Wurthner, *Angew. Chem., Int. Ed.*, 2007, **46**, 5541–5544.
37 Y. Qi, R. Xie, A. Yu, M. N. Bukhari, L. Zhang, C. Cao, H. Peng, K. Fang and W. Chen, *RSC Adv.*, 2020, **10**, 34373–34380.
38 Y. Qi, R. Xie, A. Yu, M. N. Bukhari, L. Zhang, C. Cao, H. Peng, K. Fang and W. Chen, *RSC Adv.*, 2020, **10**, 34373–34380.
39 J. D. Halverson, C. Maldarelli, A. Couzis and J. Koplik, *J. Chem. Phys.*, 2008, **129**, 827.
40 S. Khan and J. K. Singh, *Mol. Simul.*, 2014, **40**, 458–468.
41 J. Yang, H. Zhou, L. Wang, Y. Zhang, C. Chen, H. Hu, G. Li, Y. Zhang, Y. Ma and J. Zhang, *ChemCatChem*, 2017, **9**, 1355.
42 R. Q. Wang, K. J. Fang, Y. F. Ren, Y. W. Song, K. Zhang and M. N. Bukhari, *J. Mol. Liq.*, 2019, **294**, 111668.